mtDNA Studies: The mtDNA damage to long and short DNA was monitored by PCR. Long-range PCR was employed to coamplify long and short mtDNA fragments. PCR products were subjected to 1.6% agarose gel electrophoresis followed by staining with ethidium bromide to detect 8636- and 316-bp DNA products. A ratio between the long and short DNA fragments was calculated by measuring the band intensity with a PhosphorImager (Molecular Dynamics, Sunny-vale, CA). For long PCR the primers were as follows: sense: 5'-AGTGCATACCGCCAAAAGA-3' and antisense: 5'-TCTAGAGCCCACTGTAAAG-3'. The primers for short PCR were as follows 5'-ATGGTCTGAGCTATGATATCAA-3' (sense) and 5'-GATTTTGGCGTAGGTTGG-3' (antisense).

Assessment of mitochondrial transmembrane potential (Δψm): HK-2 cells were transfected with Rap1b, C/EBP-β-siRNA or PGC-1α-siRNA and plated on 35-mm glass-bottom culture dishes, and maintained at 37°C in a serum free medium for 12 hrs. Then they were treated with HG treatment for 3 days in a defined medium. Following which the cells were transferred to a phenol red-free DMEM (Life-Tech, Carlsbad, CA). 10 nM of TMRE dye (Molecular Probes) added to the medium and cells maintained at 37°C for 10 minimums. Following a brief wash with PBS the mitochondrial Δψm in intact cells was assessed by FACS analyses. In addition, Confocal microscopy was performed using a wavelength of 582 nm, and the data from four different experiments were analyzed. In isolated mitochondria from renal tissues, the Δψm was gauged following a load of rhodamine 123 (Rh123) in a medium containing 150 mM sucrose, 5 mM $MgCl_2$, 5 mM KH_2PO_4, 20 mM potassium-HEPES, pH 7.4 in the presence or absence of 10 mM glutamate and 5 mM malate at 28°C. Afterwards, the ratio of fluorescence at 520-nm and 497-nm excitation wavelengths and 529-nm emission wavelength was calculated, as further detailed in previous publications (Biochica et Biophysica Acta. 850:436-448, 1986; Am J. Physiol Regul Integr Comp Physiol. 290:R1616-R1625, 2006).

Mitochondrial enzyme activities: Manganese superoxide dismutase (Mn-SOD) activity and CuZn-SOD activity was determined in mitochondrial fractions of kidney tissues using Superoxide Dismutase [SOD] Activity Assay Kit Alexis® Biochemicals, ABL-SOD-560-KI01). Superoxide Dismutase [SOD] Activity Assay Kit not only measures total SOD activity but also can be used to distinguish CuZn-SOD or Mn-SOD activity separately. The mitochondrial catalase activity was measured using Catalase Activity Colorimetric/
Fluorometric Assay Kit (BioVision, Inc). The levels of glutathione peroxidase (GSH-Px) were determined using the Glutathione Peroxidase (GSH-PX) Assay Kits (Biocompare, Inc). All assays above were performed by following the vendors' guidelines.

Examination of fragmentation and length of long-axis of mitochondria: Kidney tissue blocks of ~1 mm^3 size were diced from each kidney cortex for standard Electron Microscopy processing. Thin sections (0.5 um) were prepared from EPON embedded tissue blocks and examined by a transmission electron microscope operating at 60 KV and mitochondrial abnormalities delineated. To determine mitochondrial fragmentation several contiguous (side-by-side) digital images were generated. Percentage of cells that had less than 1% long filamentous mitochondria were reflective of mitochondrial fragmentation. To determine the length of long-axis of mitochondria, digital images were generated. Then, the length of individual mitochondria in a cell was measured by using NIH Image software (http://rsbweb.nih.gov/ij/). For each cell, approximately 25 mitochondria were measured to determine the percentage distribution of mitochondria with various lengths, either ranging 0

2 μm or >2 μm, and the latter measurement was considered to be representative of elongated filamentous mitochondria.

PGC-1α gene promoter analysis: Various deletion constructs of PGC-1α promoter were generated by PCR. The PCR products were cloned into XhoI- and Hind III-digested pSEAP2-Enhancer plasmid vector (CLONTECH) and confirmed by nucleotide sequencing. HK-2 cells were transfected with various plasmid deletion constructs using Lipofect AMINETM 2000 reagent. Minimal promoter activity of the PGC-1α promoter activity was measured in the supernatants of the cell cultures using a Great EscAPeTM SEAP fluorescence detection kit (CLONTECH). The activities of various deletion constructs were expressed as the percentages of the activity in the deletion construct with the highest promoter activity, which was designated as being 100%.

Preparation of nuclear extracts and electrophoretic mobility assays (EMSA): Nuclear extracts used in EMSAs assays from HK-2 cell were performed as follows. Briefly, the nuclear extracts (10μg) were incubated with 1–3 μg/μl poly (dI-dC), 50 mM Tris-HCl, 750 mM KCl, 2.5mM EDTA, 0.5% Triton X-100, 62.5% glycerol (v/v), 1mM DTT) and 40,000 CPM of [γ-32P] dATP end-labeled oligonucleotides containing putative CRE (cAMP response elements) within the -146 to -132 bp region of the hPGC-1α promoter corresponding to GGCTGCCTTTGAGTGACGTCA CAC-3'. Next, the Rap1b G12V, Rap1b M17, mutant CRE site Oligo and C/EBP-β-siRNA and/or anti-PGC-1α were then transfected or added into HK-2 cells. The samples were then subjected to native 5% acrylamide gel electrophoresis for 1.5 hrs at 250 V. The gels were subsequently treated with acetic acid/methanol/water (10:30:60) for 15 min, dried and imaged using an instant imager.

Chromatin immunoprecipitation (ChIP) analysis: ChIP analysis was performed using a transcription factor ChIP kit according to the manufacturer's instructions. Soluble chromatin was co-immunoprecipitated with anti-PGC-1α antibody or an equal amount of control rabbit IgG. Co-precipitated DNA was analyzed by qPCR, using the primer pairs used for PCR analysis. The primer sequences spanning -2160 to -1938 region were as follows: Sense - 5'-GGCTTCTGTTTGCCTTGCTCAG-3' and antisense - 5'-ATACTGATACTG
CG ATTGTTA AGCG-3'. This region of amplification contains FoxO1-
dependent binding element (FoxO1-DBE) in the Catalase enzyme promoter (NC-005102.2). The PCR was also performed for MnSOD with following sequences as: Sense - 5'-GTTCCTCTTCGCCTGACTGTT-3' and antisense 5'-CTGAA CCGTTTCCGTTGCTT-3'. The GAPDH promoter was also analyzed by ChIP in parallel as a control. Finally, the relative ChIP units were defined by the ratio of ChIP DNA to input DNA following densitometry.

SUPPLEMENTARY DATA

Supplementary Table 1.（Primer Sequence）

Primer Name	Primer Sequence
Human NRF-1	Sense 5'-gatggcactgtctcacttatcc-3'
	Antisense 5'-CTGATGCTTGCGTCGTCT-3'
Human Catalase	Sense 5'-TCG AGC ACG GTA GGG ACA GTT CAC-3'
	Antisense 5'-TCC GGG ATC TTT TTA ACG CCA TTG-3'
Human GSH-Px	Sense 5'-GCG GCG GCC CAG TCG GTG TA-3'
	Antisense 5'-GAG CTT GGG GCT GGT CAT AA-3'
Human Mn-SOD	Sense 5'-CTCCCCGACCTGCCCTACGACTAC-3',
	Antisense 5'-AAACCAAGCCAACCCCAACCTGAG-3'
Human mtTFA	Sense 5'-TGTTCACAATGGATAGGCAC-3'
	Antisense 5'-TCTGGGTTTTCCAAAGCAAG-3'
Human β-actin	Sense 5'-TCACCCACACTGTGCCCATCTACGA-3'
	Antisense 5'-CAGCGGAACCGCTCATTGCCAATGG-3'
Rat NRF-1	Sense 5'- TTACTCTGCTGTGGCTGAT GG -3'
	Antisense 5'-CCTCTGATGCTTGCGTCGTCT-3'
Rat mtTFA	Sense 5'-TTG GGA TTG GGC ACA AGA AG-3'
	Antisense 5'-AAC CCG CAC GAA ACT GTC A-3'
Rat Mn-SOD	Sense 5'-GCGACCTAC GTGAACAATCTGAACG-3'
	Antisense 5'-TCAATCCCCAGCAGTGGAATAAGG-3',
Rat Catalase	Sense 5'-ATTGCCGTCCGATTCTCC30-3'
	Antisense 5'-CCAGTTACCATCTTCAGTGTAG-3'
Rat GSH-Px	Sense 5'-GTCCACCGTGTATGCCTTC-3'
	Antisense 5'-CTCTTCATTCTTGCCATTCTCC-3'

SUPPLEMENTARY DATA

Supplementary Figure 1. Rap1 inhibits Cyto C release, Drp1 translocation into the mitochondria, modulation of pro-caspases 3 and 9, and cleaved-caspase 3 expression and anti-oxidative genes in kidneys of STZ induced diabetes. (Panel A) Western blots of tubular extracts of kidney tissues in each group showing protein expression of pro-caspase 3, cleaved-caspase 3 and pro-caspase 9, mCyto C and phosphorylation of Drp-1 (p-Drp-1 at Ser656). (Panel B) Western blots of mitochondrial fractions from kidney tissues showing protein expression of mCyto C and p-Drp1 at Ser656. (Panel C) The bar graphs represent the quantification of average band intensity of panel A (A1 – A5) and Panel B (B1 & B2), N=4. (Panel D) By real time PCR showing mRNA expression of Catalase, MnSOD, GSH-Px, RNF1 and mtTFA in kidneys of each group. (Panel E) Western blots of mitochondrial fractions from kidney tissues showing protein expression of Mn-SOD, Catalase, GSH-Px, NRF1 and mtTFA. (Panel F) Quantification of average band density from four Western blot analyses included in Panel E. (Panel G) Relative activities of antioxidant enzymes (Catalase, Mn-SOD, CuZn-SOD and GSH-Px) in kidney tissues in various groups. *P <0.01 versus control, $^{\#}$ <0.01 versus STZ group.

SUPPLEMENTARY DATA

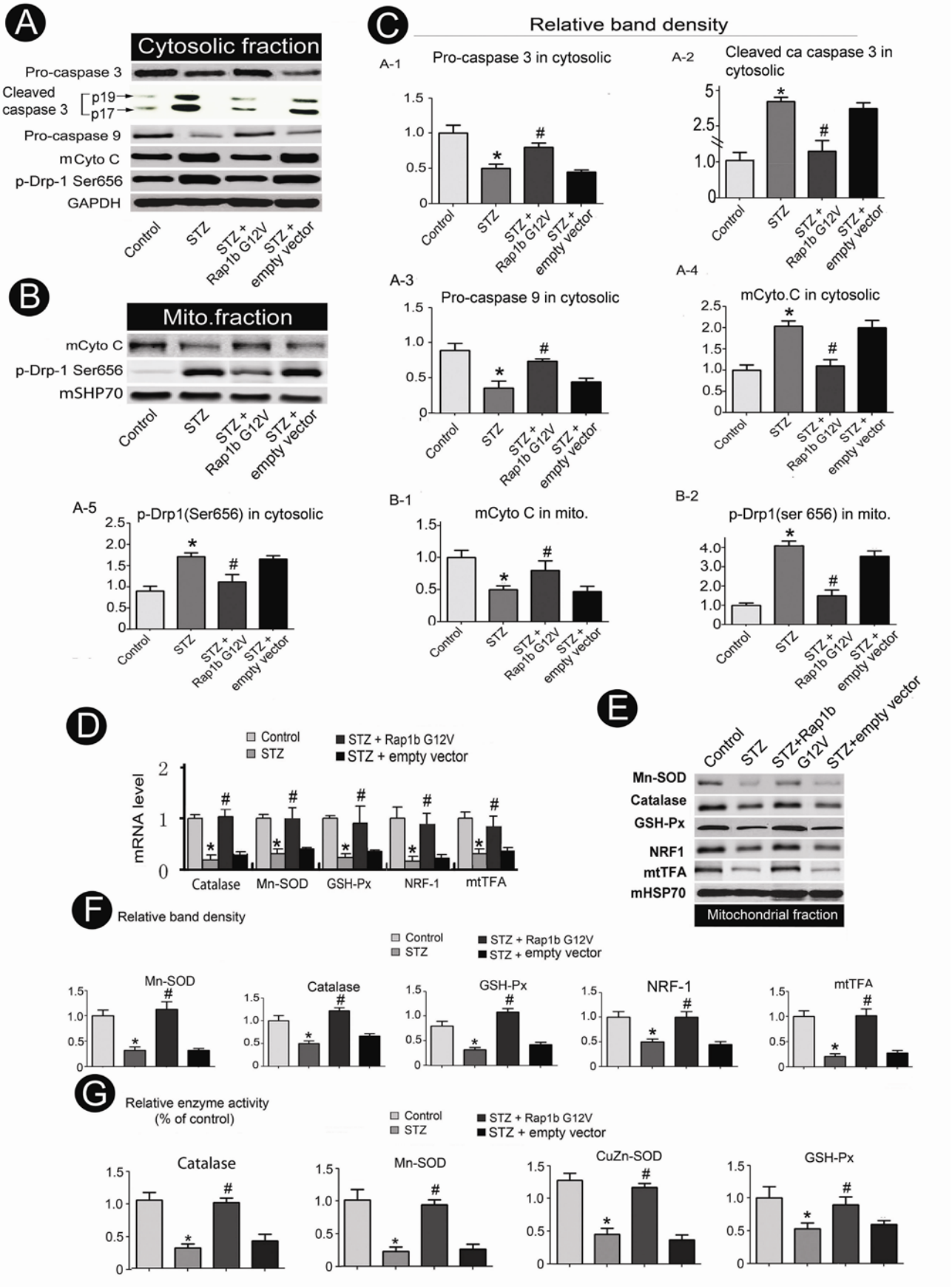

SUPPLEMENTARY DATA

Supplementary Figure 2. Decreased expression of Rap1b and Rap1b GTP activity in HK-2 cells exposed to high glucose ambience. (Panel A) By cell immunofluorescence microscopy a dose-dependent decreased expression of Rap1b in HK-2 cells treated with high glucose was observed. Mannitol (30 mM) was used as an osmolality control. (Panels B & C) Western Blot/activity assay show that the expression of Rap1b GTP activity decreased in a dose and time-dependent manner in HK-2 cells treated with D-glucose. (Panels D & E) Bar graphs represent the quantification of relative band intensity of blots depicted in panels B & C. Values are means +/- SE, N =4, *P <0.05, **P <0.01 vs. control.

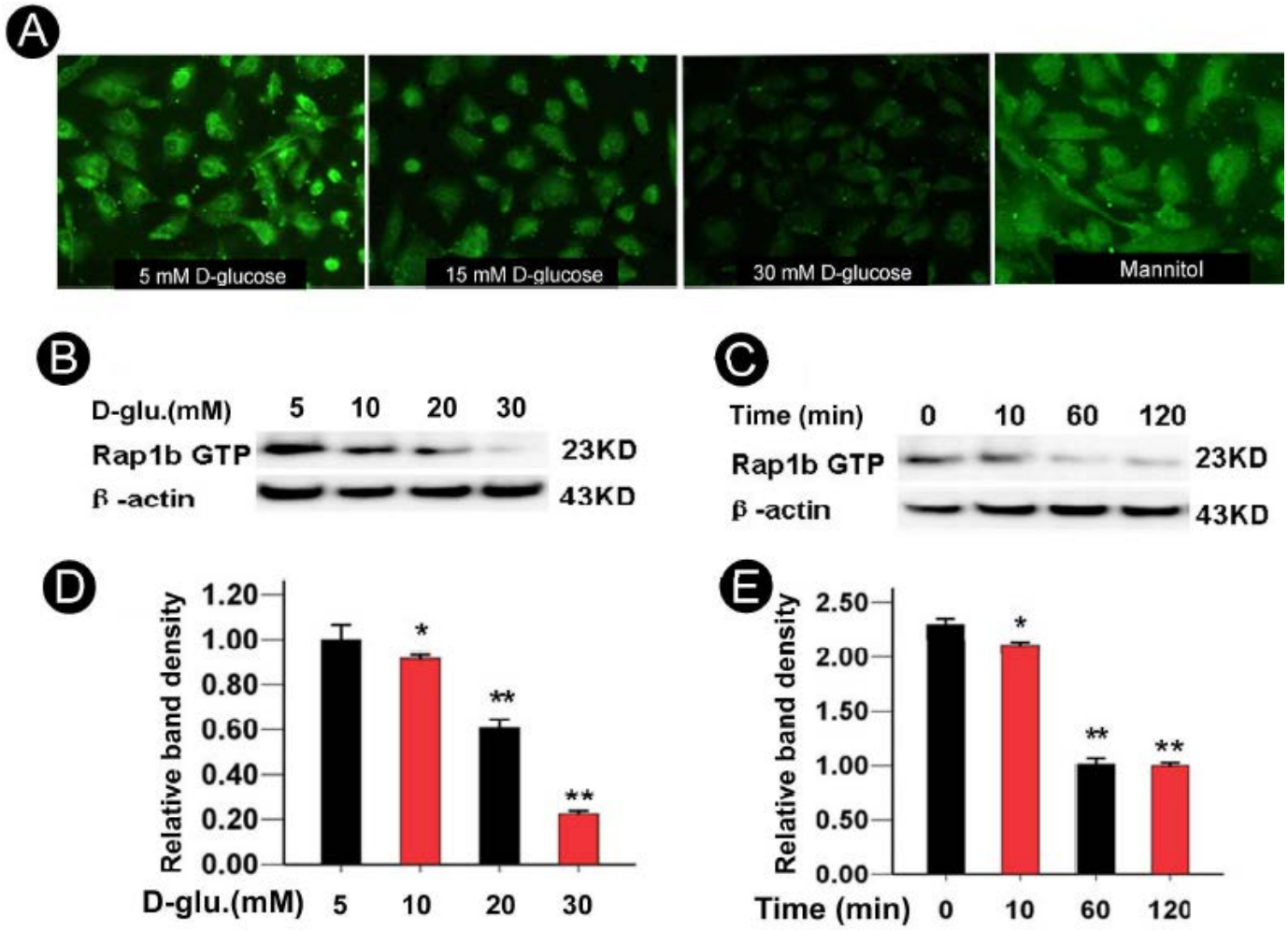

SUPPLEMENTARY DATA

Supplementary Figure 3. Effect of Rap1b on HG induced membrane potential (ΔΨm) and mtDNA fragmentation in HK2 cells. (Panel A) Confocal microscopy of HK2 cells transfected with Rap1b G12V, CEBP-β siRNA and PGC-1-α siRNA, then subjected to different concentrations of D-Glucose for 168 hrs and then stained with TMRE. Lower panels depict the area outlined by rectangles of the upper panels. (Panel B) Flow cytometric analyses of HK-2 cells treated with different concentrations of D-glucose and then stained with TMRE. (Panel C) Overexpression of Rap1b G12V led to an amelioration of TMRE fluorescence to baseline, while pretreatment with C/EBP-β or PGC-1-α siRNA led to only a partial reversal of amelioration. (Panel D) High molecular weight mtDNA expression was measured by Real time PCR in cells subjected to different concentrations of glucose for 24, 96 and 168 hrs. (Panel E) Treatment of HG for 168 hrs induced increased DNA fragmentation, which was reduced with the transfection with Rap1b G12V; however, this normalizing affect was partially reduced with the pre-treatment of CEBP-β siRNA and PGC-1-α siRNA. *P <0.01 versus 5 mM-D-glucose; $^{\&}$P <0.01 versus 15mM D-glucose; $^{@}$P <0.01, $^{\#}$P <0.05 versus 30 mM D-glucose + Rap1bG12V, N =6.

SUPPLEMENTARY DATA

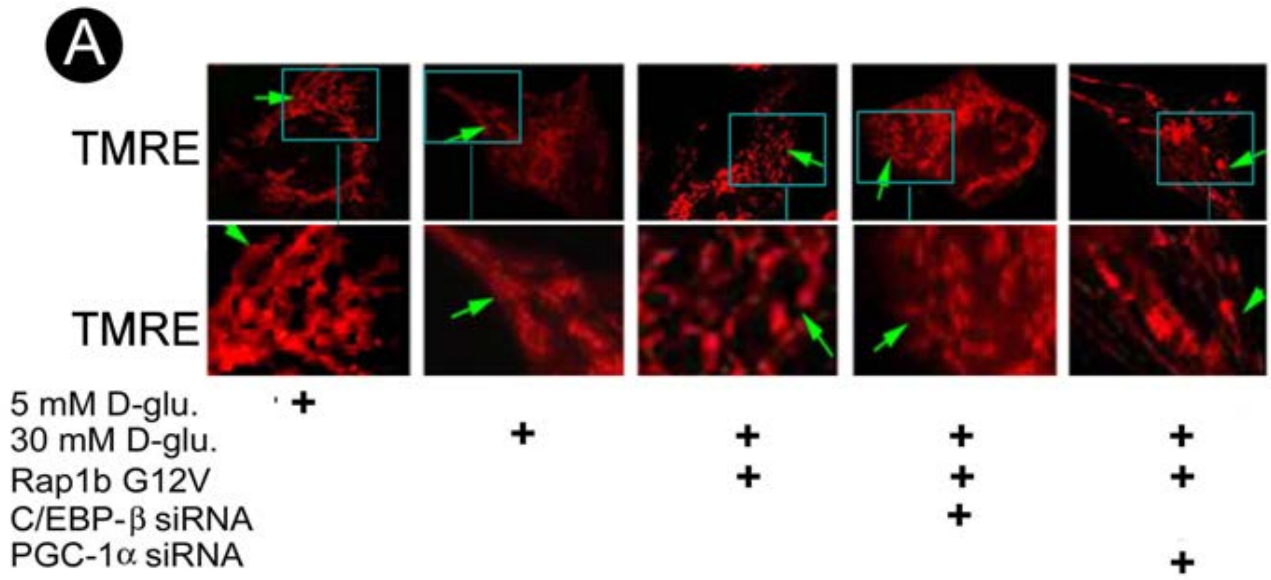

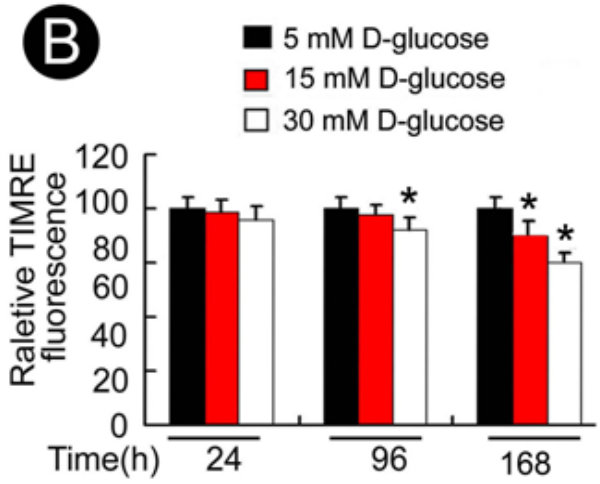

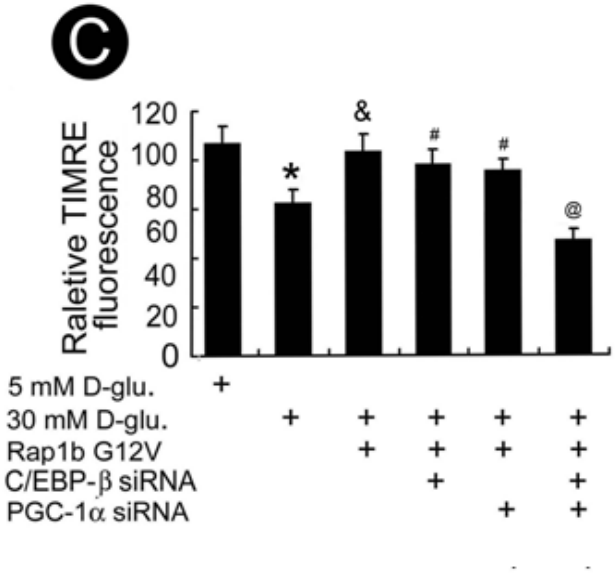

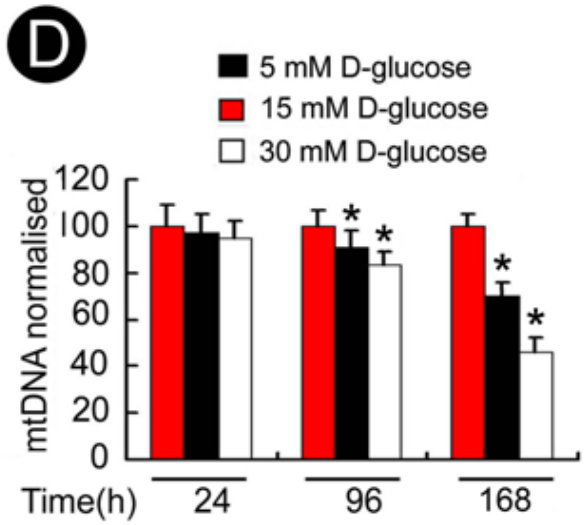

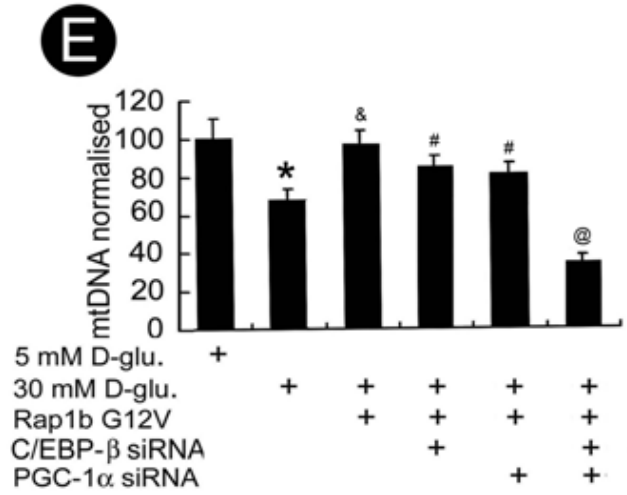

SUPPLEMENTARY DATA

Supplementary Figure 4. Effect of Rap1b on the expression of anti-oxidative genes, NRF-1 and mtTFA and their activity in HK-2 cells exposed to HG. (Panel A) Real-time PCR analysis showing that overexpression of Rap1 G12V in HK2 cells ameliorates HG-mediated reduction in mRNA levels of Catalase, Mn-SOD, NRF-1 and mtTFA; while these effects were blocked with the pre-treatment of PGC-1α and C/EBP-β siRNA. (Panel B) Similar results were seen for protein expression, as assessed by Western Blotting procedures. (Panel C) The bar graphs representing the relative intensity of bands of Western blot analysis, N=4. (Panel D) The bar graphs representing enzyme activity of antioxidant proteins in HK-2 cell exposed to HG with or without transfection of Rap1b G12V and pre-treatment with CEBP-β siRNA or PGC-1-α siRNA. Values are means +/- SE. N=4, *P <0.01 versus 5 mM D-glucose; $^{\&}$P <0.01 versus 30 mM D-glucose; $^{\#}$ P <0.01 versus 30 mM D-glucose + Rap1b G12V.

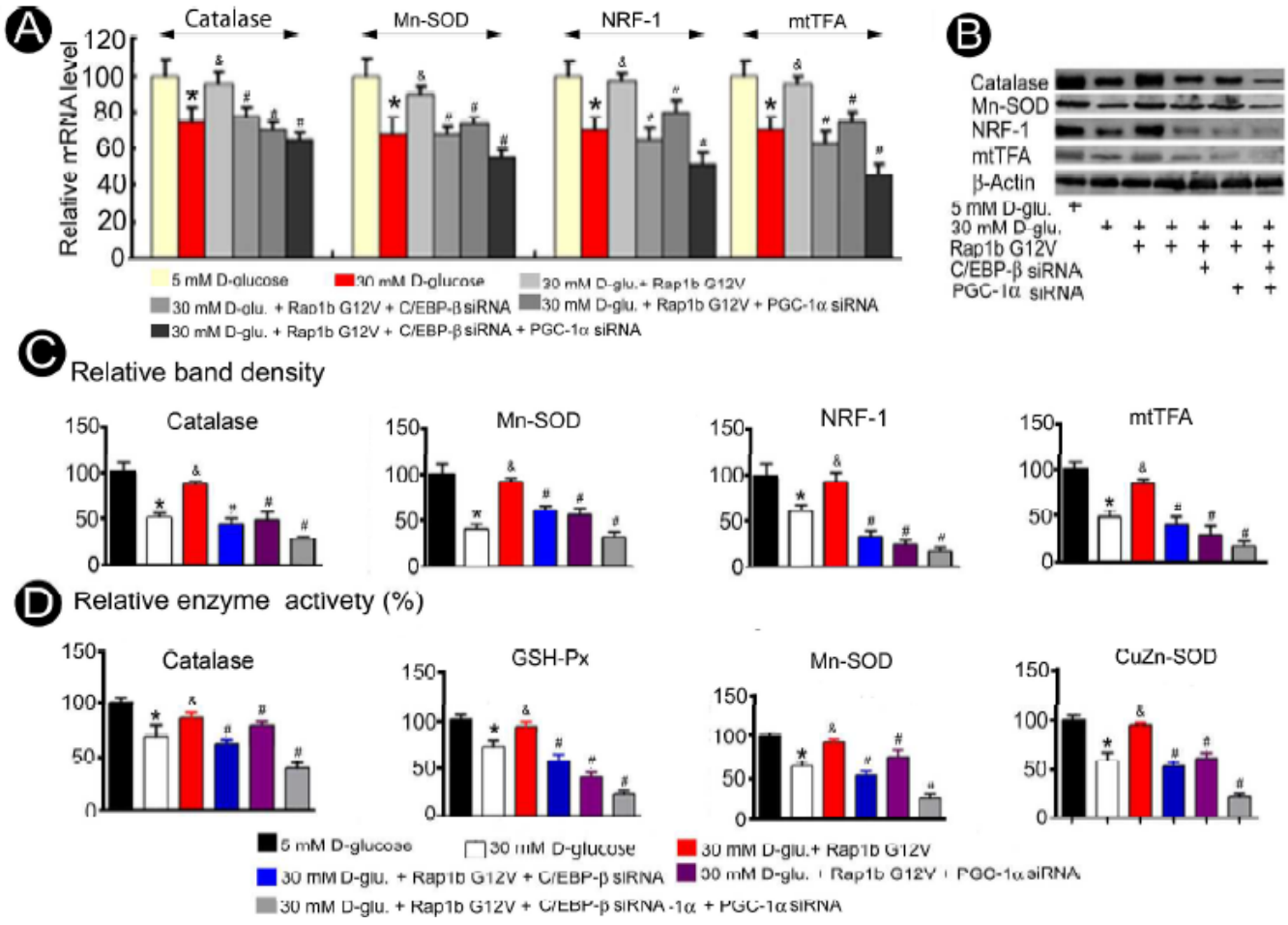

SUPPLEMENTARY DATA

Supplementary Figure 5. Schematic sketch of conceivable cellular events following exposure to HG ambience and overexpression of Rap1bG12V in renal tubular cells. HG ambience led to an activation of Rap1 GAP and reduced Rap1 GTPase activity in renal tubular cells which inhibits ERK1/2 - C/EBP-β:PGC-1α nuclear translocation, and this in turn reduces the expression of mitochondrial antioxidant genes, e.g., Catalase and Mn-SOD as well as mitochondrial biogenesis genes, e. g., NRF1 and mtTFA. This eventually causes mitochondrial dysfunctions, including release of mitochondrial Cytochrome C, activation of caspases, fragmentation of DNA and cellular apoptosis. Conceivably, transfection of GTPase Rap1b interrupted the signaling pathway to ameliorate mitochondrial dysfunctions that occurs following HG ambience. In addition, overexpression of Rap1b possibly blocks the phosphorylation and mitochondrial translocation of Drp1 protein that modulates mitochondrial dynamics and reduces the generation of ROS production and consequential cellular damage.